Applied Physics B (2023) 129:133
https://doi.org/10.1007/s00340-023-08078-9

Applied Physics B
Lasers and Optics

RESEARCH

Laser irradiation of differently aged carbon nanoparticles: effect on optical properties

F. Migliorini[1] · S. Belmuso[2] · D. Ciniglia[1] · R. Dondè[1] · S. De Iuliis[1]

Received: 20 February 2023 / Accepted: 14 July 2023 / Published online: 26 July 2023

Abstract

The effect of laser irradiation on carbon nanoparticles of different maturity sampled from a premixed flame is investigated. To this purpose, extinction and laser-induced incandescence measurements are carried out on pristine and pre-irradiated nanoparticles. From extinction measurements, a spectral trend of the absorption coefficient of the particles is retrieved. Moreover, two-color laser-induced incandescence versus fluence is used to investigate the behavior of signal and temperature fluence curves in the different conditions under analysis. By coupling these results, interesting outcomes are obtained depending on the nature (nascent vs mature) of the particles. For nascent particles, a significant shift of the fluence curves is observed for the pre-irradiated particles, suggesting an increase in the absorption efficiency. However, no changes in the spectral trend of the absorption coefficient are observed from extinction measurements. On the contrary, for mature particles the absorption properties are strongly affected by irradiation resulting in an increase in the absorption efficiency in the spectral region below 600 nm. Moreover, a decrease of the temperature at the plateau regime for pre-irradiated mature particles towards the temperature value reached by nascent particles is observed. Two processes, namely fragmentation and sublimation followed by nucleation of new particles are suggested to occur under laser irradiation, especially for mature carbon nanoparticles.

1 Introduction

Laser-induced incandescence employed in nanoparticle-laden aerosol is a powerful diagnostic tool to gain information on dimension and volume fraction of the particles under analysis [1]. Time-resolved LII technique is in fact widely applied to carbon as well as other synthetic nanoparticles [2–6]. However, referring to carbon nanoparticles, the response of nanoparticles to nanosecond laser irradiation is strictly dependent on particle properties, which can be different according to their structure and morphology, composition and aging stage [7–10]. In addition, under laser irradiation, particles can undergo significant changes in structure and composition depending on the laser fluence used, which can ultimately affect their optical properties. Therefore, it is noticeable that for the application of the technique, the knowledge of the "initial" optical properties and their changes under laser irradiation represents a significant problem to consider.

According to the findings reported in the literature, different processes are proposed to describe the effect of laser irradiation, which however are related to the specific conditions under analysis (temperature, fuel used, combustion conditions and aging stage).

In most of the works, thermal annealing was considered to play a prominent role in the change of carbon particles nanostructure, improving the order of larger graphitic layers and resulting in an increase in absorption efficiency [11–13]. This was already proposed by Vander Wal et al. in the '90 s [11, 12], with their measurements performed in a premixed flame. They observed a significant graphitization and formation of onion-like structures. Such behavior was confirmed by Apicella et al. [13] in methane and ethylene flames. They coupled HRTEM, UV–Vis spectroscopy and Raman spectroscopy and were able to differentiate laser modification according to the initial structure of nascent and mature nanoparticles.

To stress the changes in particles inner structure, the effect of multiple laser-shot irradiation was studied on particles sampled from diffusion and premixed flames [14].

✉ S. De Iuliis
silvana.deiuliis@cnr.it

[1] Institute of Condensed Matter Chemistry and Technologies for Energy, CNR-ICMATE, Via Cozzi 53, 20125 Milan, Italy

[2] AMAT srl, Mobility, Environment and Territory Agency, Via Tommaso Pini 1, 20134 Milan, Italy

In particular, a graphitization process was observed on particles sampled from the diffusion flame and analyzed via TEM, resulting in a change in the refractive index and a related increase in the absorption coefficient.

More recently, in the work by Török et al. [15] the same conclusion was obtained by performing LII measurements at 532 nm and 1064 nm excitation wavelengths on laser-heated carbon nanoparticles produced with a mini-CAST (propane-air co-flow diffusion flame operation mode). By analyzing the fluence curves, they observed a significant increase in the LII signal of pre-heated nanoparticles, suggesting the occurrence of thermal annealing on the particles under analysis.

Another interesting description of the physical and chemical processes occurring under laser irradiation was proposed by Michelsen et al. [16]. According to their measurements, the vaporization of carbon fragments results in nucleation and formation of new particles.

In line with these results, wavelength-resolved extinction measurements, Raman spectroscopy and particle size distribution measurements performed on pristine and pre-irradiated carbon nanoparticles sampled from a quenched diffusion flame are reported in [17]. The significant variation in the optical properties of pre-irradiated compared to pristine nanoparticles was interpreted considering a strong fragmentation of the aggregates and/or formation of new particles [17] as detected from particle size distribution measurements.

Moreover, the influence of laser irradiation on particles sampled from a premixed flame was further investigated in a double pulse experiment, where LII signal and peak temperature versus laser fluence were compared in the case of pristine and pre-irradiated nanoparticles [18]. It was found that at low laser fluence, while for nascent particles signal and LII peak temperature increase comparing pristine and pre-irradiated nanoparticles, no significant changes were detected for mature carbon particles. In this work, however, a variation of the optical properties under laser irradiation was not considered in the analysis of LII data.

The novelty of this work is the investigation of the effect of laser irradiation on the spectral behavior of the optical properties of carbon nanoparticles sampled from a premixed flame. This study is performed on nanoparticles sampled at different heights above the burner surface, considering that at low height particles are regarded as nascent and become mature increasing the sampling height [13, 18]. Extinction measurements are carried out on pristine and pre-irradiated nanoparticles and coupled with laser-induced incandescence measurements. In particular, LII peak signal and temperature versus laser fluence are compared for pristine and pre-irradiated particles. Combining the two techniques it is possible to gain information on the processes happening under laser irradiation and the subsequent effects on particles properties and structure, which is pivotal for the correct application and interpretation of optical diagnostic techniques.

2 Experimental setup

In the present study, two-color LII and extinction measurements are conducted on pristine and pre-irradiated carbon nanoparticles by combining the experimental setups used in [18] and [19, 20]. A schematic of the experimental apparatus is shown in Fig. 1.

Carbon nanoparticles are produced in a rich premixed ethylene/air flame stabilized on a water-cooled sintered bronze McKenna burner by using a stainless-steel 60 mm diameter plate positioned at 30 mm height above the burner. The cold gas velocity is set at 10 cm/s with a carbon to oxygen (C/O) atomic ratio fixed at 0.7, corresponding to a flame equivalence ratio Φ of 2.1.

Combustion products (particles and gaseous species) are sampled from the center of the flame through a dilution probe and dried by passing through an ice trap unit, as described in previous studies [18–20]. To ensure that extinction measurements are related exclusively to carbon nanoparticles and not the carrying gas, a three-way valve is used to discriminate between a particle-laden aerosol sample or a filtered aerosol sample, allowing the evaluation of the contribution of the gas phase to the absorption measurements [19, 21]. Particles are sampled at 8 mm, 10 mm and 14 mm above the burner surface to study particles in different aging conditions. The sampling flow rate is set to 1 l/min.

After sampling, the aerosol flows through an irradiation unit, which consists of a glass tube (5 mm i.d., 10 cm long) where particles are pre-irradiated by a Nd:YAG laser beam (Quantel, Big Sky, CFR 400, 1064 nm, 10 Hz, top-hat beam profile). A portion of the beam is selected by means of an aperture having the same diameter as the glass tube and properly aligned in order to irradiate all the particles in the unit volume. We estimate that the percentage of the single irradiated particles spans between 70 and 85%, corresponding to laminar or plug flow condition inside the irradiation tube. However, it is worth noticing that double irradiation at the fluences under analysis slightly affect the LII signals as reported in [14]. The laser energy is varied in order to investigate the impact on particle properties. Pristine or pre-irradiated particles are then sent either into a portable in-house developed Sphere-integrated LII Spectroscopy Instrument (SiLIIS) or into an extinction unit. The SiLIIS instrument is used to performed two-color laser-induced incandescence measurements at different laser fluences. In the case of pre-irradiated particles, LII measurements are performed few seconds after the pre-irradiation laser pulse. Details on the instrument and the measurements condition are reported in [18, 22]. In the present work LII signals are collected at

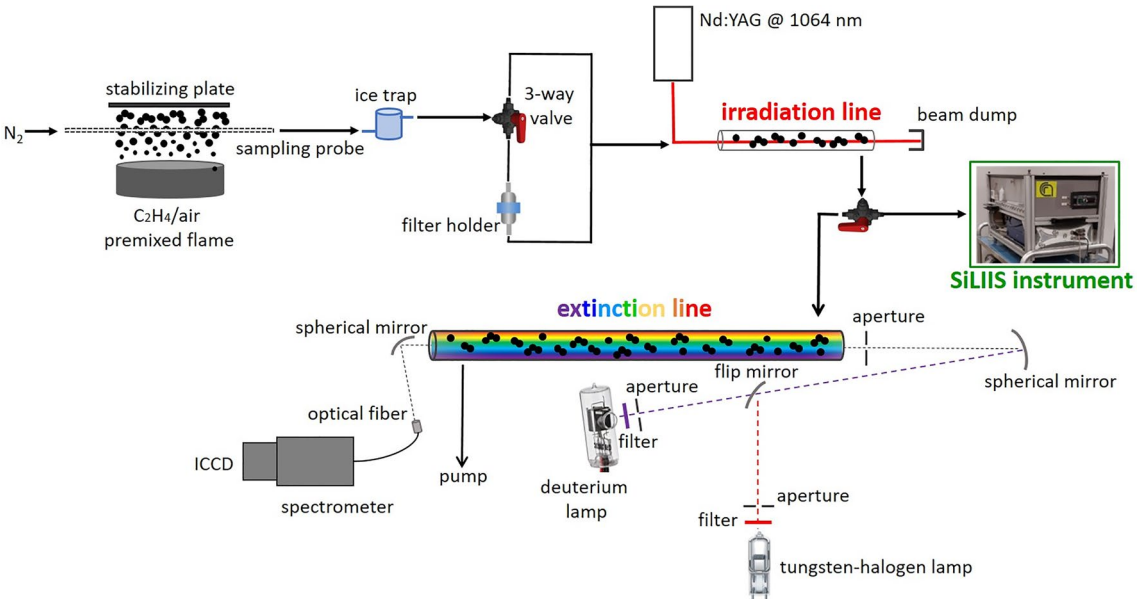

Fig. 1 Experimental set-up for extinction and laser-induced incandescence measurements

610 nm (bandwidth of 40 nm) and 700 nm (bandwidth of 60 nm). The extinction unit is similar to the one used in [19], although the measuring line is longer (450 cm) than the tube used in [19] in order to increase the sensitivity. Wavelength-resolved extinction measurements on pristine and pre-irradiated particles are performed in the 300–834 nm spectral region. To this purpose, two different light sources are used:

- a deuterium lamp (63,379 Oriel 30 W) in the 300–450 nm range
- a tungsten halogen lamp in the 450–834 nm range.

A flip mirror is used to select alternately the two lamps. The total extinction spectra are obtained by combining consecutive spectral ranges, taking advantage of the small overlap of wavelengths, and avoiding second-order effects by using different long pass filters. The signal intensity is measured with a Czerny-Turner spectrograph (Shamrock 303i, 150 grooves/mm) coupled with an ICCD camera (iStar 334 T, Andor Technology). Each spectrum results from an accumulation of 1000 individual spectra to reduce shot noise.

3 Experimental procedure

In order to investigate the effect of laser irradiation on the absorption properties, extinction measurements on pristine and pre-irradiated carbon nanoparticles are performed. In this last case, laser fluence of 220 mJ cm^{-2} and 400 mJ cm^{-2} are used for pre-irradiation.

According to the Beer-Lambert law, the spectral transmittance τ_λ, given by the ratio of transmitted and incident light intensity for each wavelength λ, can be related to the extinction coefficient $k_{ext,\lambda}$ as

$$\ln(\tau_\lambda) = k_{ext,\lambda} L \tag{1}$$

where L is the optical path length. In our case, the spectral transmittance of the particles is obtained by dividing the signal from particle-laden gas by the signal from filtered gas.

If one considers negligible the scattering contribution to the extinction coefficient, as observed in similar experimental conditions [23] and reported in the Supplementary Material (SM), the absorption coefficient can be retrieved as

$$k_{abs,\lambda} = \frac{6\pi E(m(\lambda)) f_V}{\lambda} \tag{2}$$

where $E(m)$ is the refractive index absorption function, which is a function of the wavelength-dependent refractive index. In the same equation, f_V is the particle volume fraction in the measuring volume.

Two-color laser-induced incandescence measurements are also carried out on pristine and pre-irradiated nanoparticles. In particular, in order to investigate the absorption efficiency at the excitation wavelength, the behavior of LII signals and peak temperature is analyzed as a function of laser fluence. The incandescence signals S_1 and S_2 are collected in the two spectral ranges (λ_1 and λ_2, respectively) and corrected for the absolute intensity calibration factor, which relates these signals to the absolute spectral

intensities of a calibrated light source. LII peak particle temperature is then obtained as follows

$$T = \frac{hc}{K_B}\left(\frac{1}{\lambda_2} - \frac{1}{\lambda_1}\right)\left[ln\left(\frac{S_1 E(m(\lambda_2))}{S_2 E(m(\lambda_1))}\right)\left(\frac{\lambda_1}{\lambda_2}\right)^6\right]^{-1} \quad (3)$$

where c is the speed of light, h is the Planck constant and K_B is the Boltzmann constant. For the refractive index absorption function at the two wavelengths, the values obtained from the absorption coefficients (see Eq. (2)) for pristine and pre-irradiated nanoparticles are used. In the following we refer to temperature as the temperature at the LII peak.

4 Experimental results

In Fig. 2 the absorption coefficients of pristine and pre-irradiated nanoparticles at 220 mJ cm^{-2} and 400 mJ cm^{-2} versus wavelength are reported for the three heights under analysis.

The spectra are normalized at 750 nm. The uncertainty of the measurements is shown as a shaded area on the corresponding absorption spectrum. Details on the measurements uncertainties are given in SM2. While at 8 mm height, no significant effect of laser irradiation is detected comparing the absorption coefficient of pristine and pre-irradiated nanoparticles, a change in the spectral behavior is observed for the other two heights under analysis, depending on the pre-irradiating fluence. In particular, at 10 mm height, the absorption coefficient spectral behavior of pristine nanoparticles is similar to the one of particles pre-irradiated at 220 mJ cm^{-2}, while it increases in the spectral region below 600 nm in the case of particles pre-irradiated at 400 mJ cm^{-2}. Finally, at 14 mm height, a more significant dependence on the pre-irradiating fluence is observed: the absorption spectrum begins to change already at 220 mJ cm^{-2} and varies more significantly at 400 mJ cm^{-2}.

As a first analysis, one can deduce that the absorption efficiency of the pristine particles at the laser excitation wavelength strongly affects the spectral behavior of the absorption coefficient of the pre-irradiated nanoparticles. In particular, at 8 mm, where nascent carbon particles are sampled, a low absorption coefficient of the pristine particles results in no effects of laser irradiation on particles absorption properties. On the contrary, going towards a more mature nature of the nanoparticles sampled at higher height above the burner surface, a higher absorption coefficient at 1064 nm results in an increasing effect on the optical properties of the particles with increasing the pre-irradiating fluence.

In Fig. 3 the peak LII signal collected at 610 nm wavelength is reported versus laser fluence in logarithmic

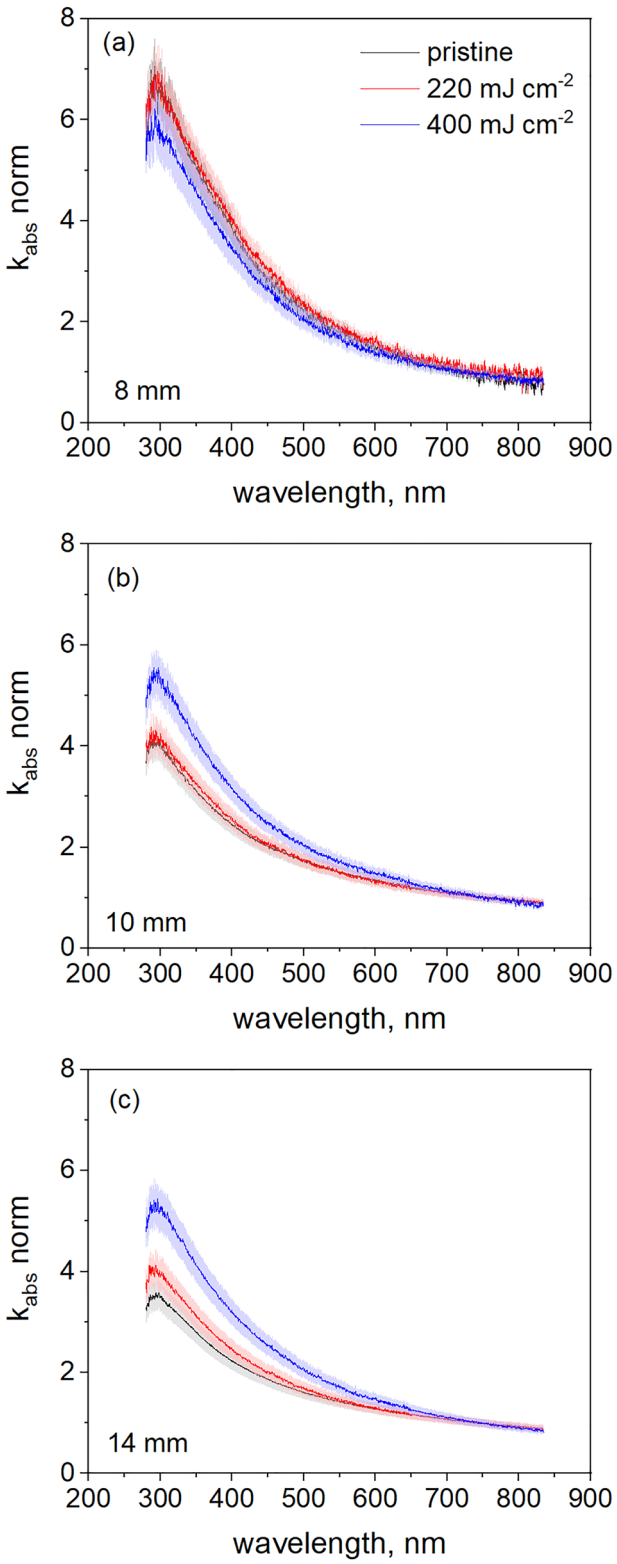

Fig. 2 Absorption coefficient versus wavelength of pristine and pre-irradiated nanoparticles at 220 mJ cm^{-2} and 400 mJ cm^{-2}. Particles are collected at 8 mm (**a**), 10 mm (**b**) and 14 mm (**c**)

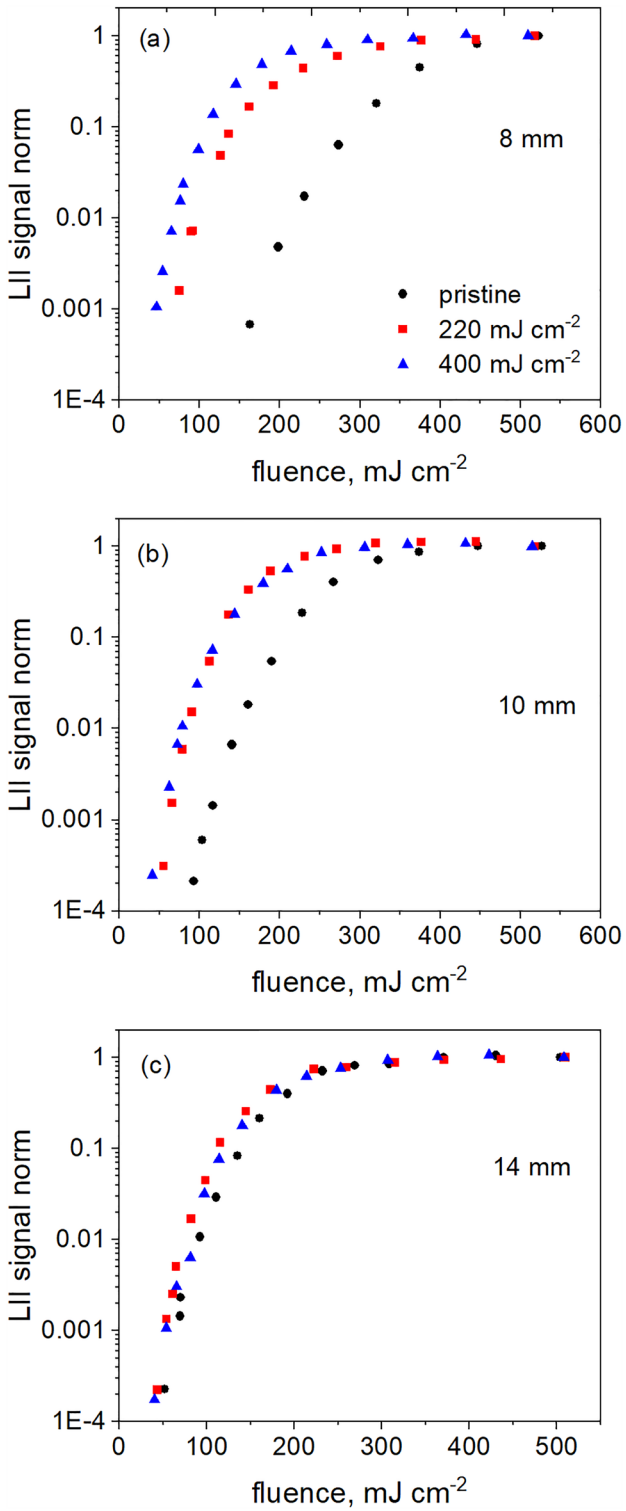

Fig. 3 Peak LII signal (collected at 610 nm) versus fluence of pristine and pre-irradiated nanoparticles sampled at 8 mm (**a**), 10 mm (**b**) and 14 mm (**c**). Curves are normalized to the highest fluence for each sampling height. The laser fluences used for pre-irradiation are: 220 mJ cm^{-2} and 400 mJ cm^{-2}

scale for particles sampled at 8 mm (a), 10 mm (b) and 14 mm(c) height. The curves are normalized to the highest fluence for each sampling height.

In agreement with our previous results [18], while at 14 mm height the fluence curves of pristine and pre-irradiated nanoparticles are very close, a substantial difference is observed for the LII measurements carried out at 8 mm. In particular, at this sampling height, the fluence curve of pre-irradiated nanoparticles is shifted towards low laser fluences compared to the curve of pristine nanoparticles. This result suggests that laser irradiation promotes an increase of the absorption coefficient of nascent particles at the excitation wavelength.

The behavior of the fluence curves related to 10 mm height particles confirms the overall trend, meaning the shift in the low laser fluence regime comparing pristine and particles pre-irradiated at 220 mJ cm^{-2}. In this case, however, increasing the pre-irradiating fluence to 400 mJ cm^{-2}, no further changes in the fluence curve are detected. Analogous results were obtained for peak LII signals collected at 700 nm, here not reported for brevity.

By taking advantage of the spectral behavior of the absorption coefficient reported in Fig. 2 in each condition, the ratio of the refractive index absorption function at the two detection wavelengths can be evaluated and particle temperature can be retrieved by applying Eq. 3.

In Fig. 4 temperature versus fluence of pristine and pre-irradiated particles at 220 mJ cm^{-2} and 400 mJ cm^{-2} are shown for the sampling heights under analysis.

A quite complex picture of the temperature can be derived for particles of different aging conditions. As for 8 mm pristine particles, the temperature increases slowly with fluence and approaches a plateau behavior at quite high laser fluences. As for the pre-irradiated particles (at 220 mJ cm^{-2} and 400 mJ cm^{-2}) temperature exhibits a significant shift in the low laser fluence regime and reaches the same temperature as pristine nanoparticles in the plateau regime. However, the temperature at the plateau regime is less than 4000 K, which is the typical value reached by mature carbon particles. This is in agreement with the work reported in [19, 24], where measurements were performed on cold carbon particles and in flame, respectively. In both papers, in fact, a significant dependence of the temperature at the plateau regime with respect to the particles aging stages is observed.

The temperature of pristine particles sampled at 14 mm exhibits the typical trend versus fluence of mature carbon particles, with the temperature increasing with fluence in the low fluence regime and reaching a constant value of about 4000 K in the saturation regime. In the case of pre-irradiated particles at 220 mJ cm^{-2}, similar behavior in the fluence curve is observed, showing a slight shift of the temperature in the low laser fluence regime, probably occurring within the measurement uncertainties. On the contrary, considering

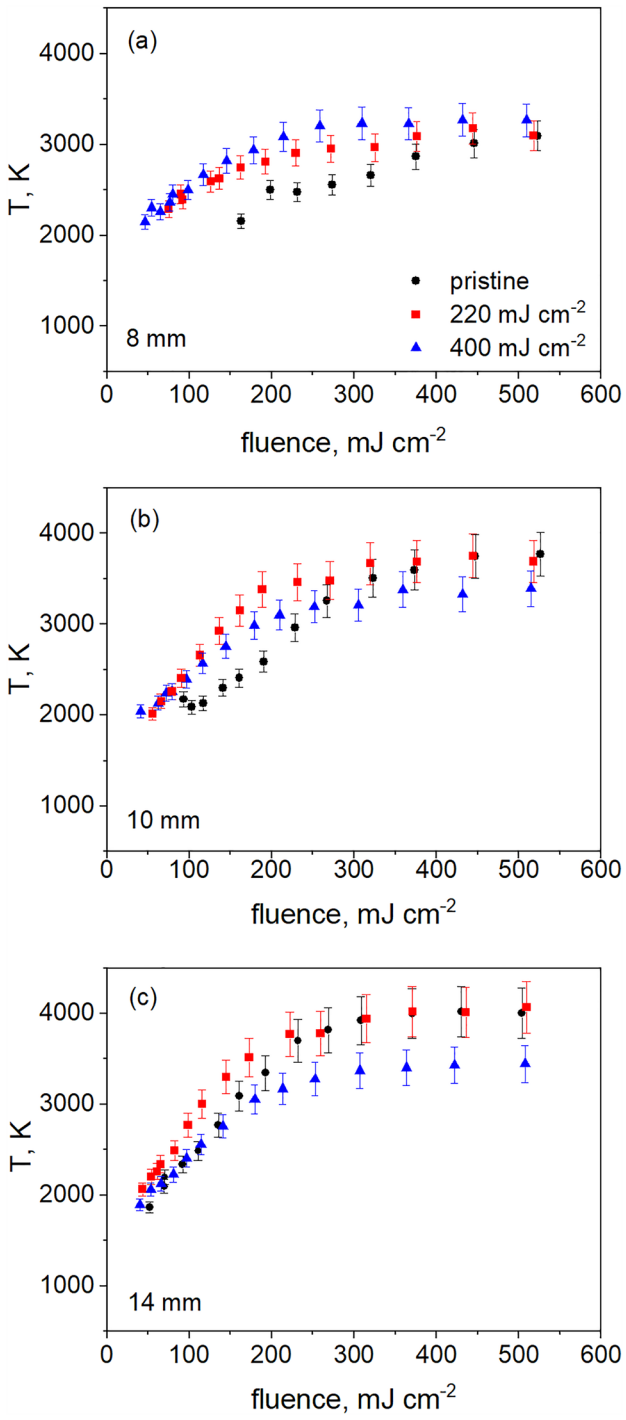

Fig. 4 Temperature versus fluence of pristine and pre-irradiated nanoparticles at 220 mJ cm^{-2} and 400 mJ cm^{-2}. Measurements are carried out at 8 mm (**a**), 10 mm (**b**) and 14 mm (**c**) sampling height. Error bars are also reported for each measurement

the particles pre-heated at 400 mJ cm^{-2}, a significant difference in the fluence curve is detected in the saturation regime, where a lower value of temperature is obtained compared to the ones of pristine nanoparticles.

Finally, pristine and pre-irradiated carbon particles sampled at 10 mm exhibit a temperature behavior intermediate with respect to 8–14 mm particles, meaning a shift in the low laser fluence regime for particles pre-irradiated at 220 mJ cm^{-2} and a reduction in the temperature at the plateau regime for particles pre-irradiated at 400 mJ cm^{-2}.

5 Discussion

By combining absorption and incandescence measurements, it is evident that the different aging stages of pristine nanoparticles account for different effects of laser irradiation. Considering nascent particles at 8 mm sampling height, although the absorption coefficient exhibits no significant changes in the spectral behavior, a substantial shift in the fluence curve is observed comparing pristine and pre-irradiated particles (Fig. 3a). This shift was already observed in the literature [7, 8, 18]. In particular, in [8] the shift was attributed to a reduction in the absorption efficiency due to the presence of a coating on the surface of the particles. Such effect was considered also in our previous work [18], but the mass of evaporated species that would justify the observed shift was evaluated as not realistic. Therefore, if happening, the evaporation of carbon species would be responsible only for a fraction of the shift. In our previous work [18] we have already observed an increase in E(m) values at 1064 nm for pre-irradiated particles compared to pristine ones. However, although the increase in the absorption efficiency at 1064 nm explains the shift in the fluence curve, such increase has to be the same at any wavelength, with no effect on the UV–Vis spectral behavior. More work is needed to shed light on the peculiar behavior of the optical properties of particles sampled at 8 mm under laser irradiation.

A different trend is detected for the other two heights under analysis. Depending on the pre-irradiating fluence, we observe a change in the spectral trend of the absorption coefficient and a decrease in the temperature at the saturation regime in the fluence curves. These effects can be ascribed to the occurrence of fragmentation processes of pristine particles and/or vaporization with formation of new ones. To stress this point we report in Fig. 5 the spectral dependence of the absorption coefficient at the heights under analysis for particles pre-irradiated at 400 mJ cm^{-2}. In Fig. 6 the LII intensity and temperature versus fluence are also shown in the same conditions.

As it can be seen from both sets of measurements (extinction and incandescence), the curves in Figs. 5 and 6 are almost overlapped, which confirms that the particles under strong pre-irradiation tend to exhibit the same trend. In other words, under laser irradiation the properties of particles sampled at 8 mm (nascent particles) do not change, while particles sampled at 10 and 14 mm are modified in

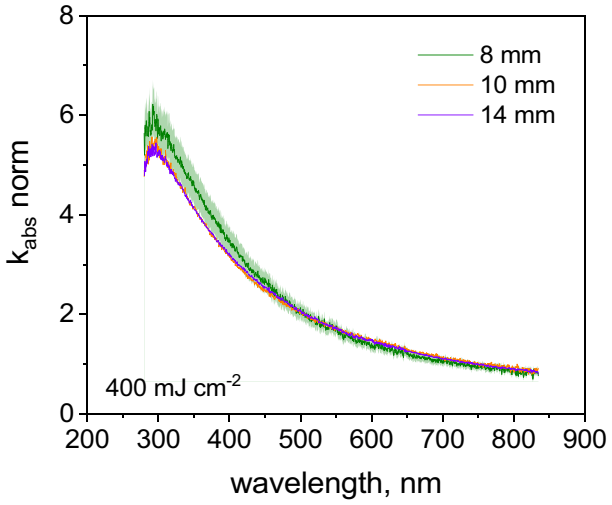

Fig. 5 Absorption coefficient versus wavelength for particles sampled at 8 mm, 10 mm and 14 mm and pre-irradiated at 400 mJ cm^{-2}. Spectra are normalized at 750 nm

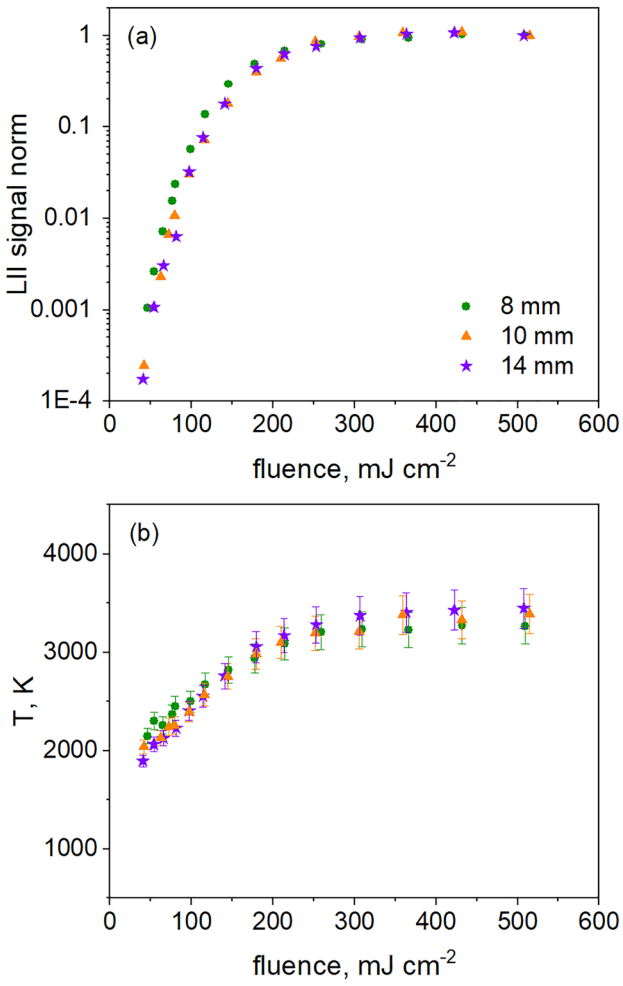

Fig. 6 Fluence curves of peak LII signal at 610 nm (**a**) and temperature (**b**) of particles sampled at 8 mm, 10 mm and 14 mm and pre-irradiated at 400 mJ cm^{-2}

their optical properties behaving as nascent particles. The same conclusion was drawn in [17] even if the analysis was performed in different conditions (diffusion vs premixed flame in this work). On the contrary, in the work by Török et al. [15] an annealing effect was considered to justify the change in LII fluence curves observed under laser irradiation. Unfortunately, particle temperature versus fluence was not reported, which could provide more insight in the interpretation of the processes involved.

In order to investigate the role of the two LII detection wavelengths, particles temperature was derived over two other pairs of LII signals, namely [530 ($\Delta\lambda = 40$ nm),700 nm] and [400 ($\Delta\lambda = 70$ nm),700 nm]. The test was performed on pristine and particles pre-irradiated at 400 mJ cm^{-2}, both sampled at 14 mm. As reported in Fig. 7, no significant differences in the temperature curves are obtained with the three pairs of wavelengths, for both pristine (a) and pre-irradiated (b) particles. These curves clearly show that scattering contribution to extinction is negligible. Moreover, the result from one side confirms the trend in temperature observed in Figs. 4 and 6 meaning the reduction of the plateau temperature for particles pre-irradiated at 400 mJ cm^{-2}, from the other side highlights the importance of using the absorption properties of pre-irradiated nanoparticles to reduce the uncertainties in temperature evaluation via two-color pyrometry. In fact, considering the absorption properties either wavelength independent or varying as $1/\lambda$ in the visible spectral region, different temperature values are obtained depending on the pairs of detection wavelengths used, as reported by Liu et al. [25, 26].

As described above the decrease in the sublimation temperature for particles pre-irradiated at 400 mJ cm^{-2} is attributed to a change in the optical properties of mature particles and the formation of new ones.

To confirm the presence of these new particles, the temporal behavior of particle temperature is analyzed. We report in Fig. 8 time-resolved temperatures at 8 mm (a) and 14 mm (b) of pristine and pre-irradiated nanoparticles at 220 mJ cm^{-2} and 400 mJ cm^{-2}. These curves are obtained from two-color LII measurements carried out at 150 mJ cm^{-2}, being the lowest available data point in the low fluence regime for pristine particles at 8 mm. Depending on the pre-irradiating fluence, particles are heated to different temperatures (for example at 8 mm temperature values are 2100 K, 2770 K and 2900 K for pristine, 220 mJ cm^{-2} and 400 mJ cm^{-2} pre-irradiating fluence, respectively). Therefore, for a direct comparison, at each of the two sampling heights, the time-resolved curves are temporally moved in order to consider the temperature decay starting from the same temperature (2100 K at 8 mm and 2800 K at 14 mm).

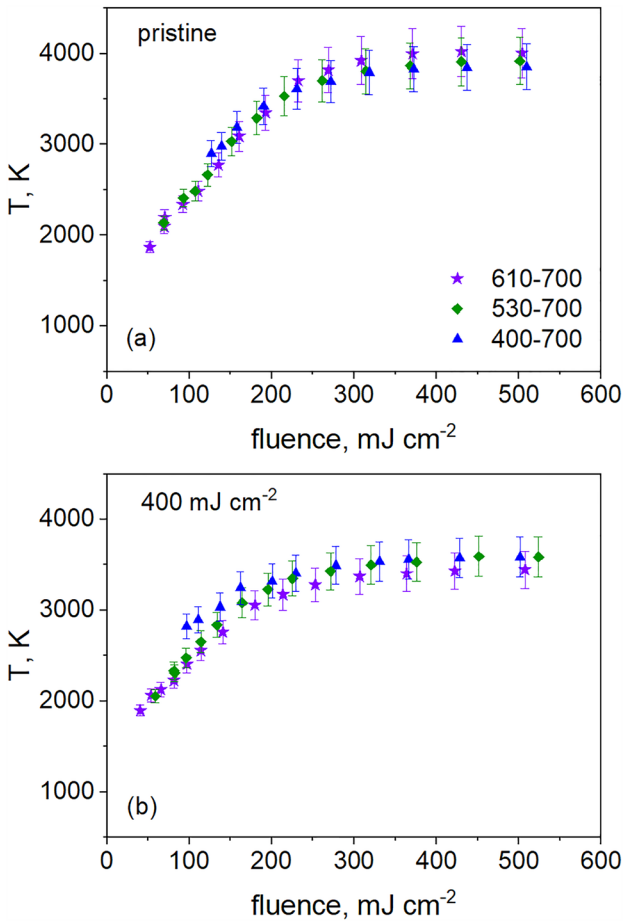

Fig. 7 Temperature versus fluence derived using three pairs of detection wavelengths. (**a**) Pristine particles and (**b**) particles pre-irradiated at 400 mJ cm^{-2}. Particles are sampled at 14 mm

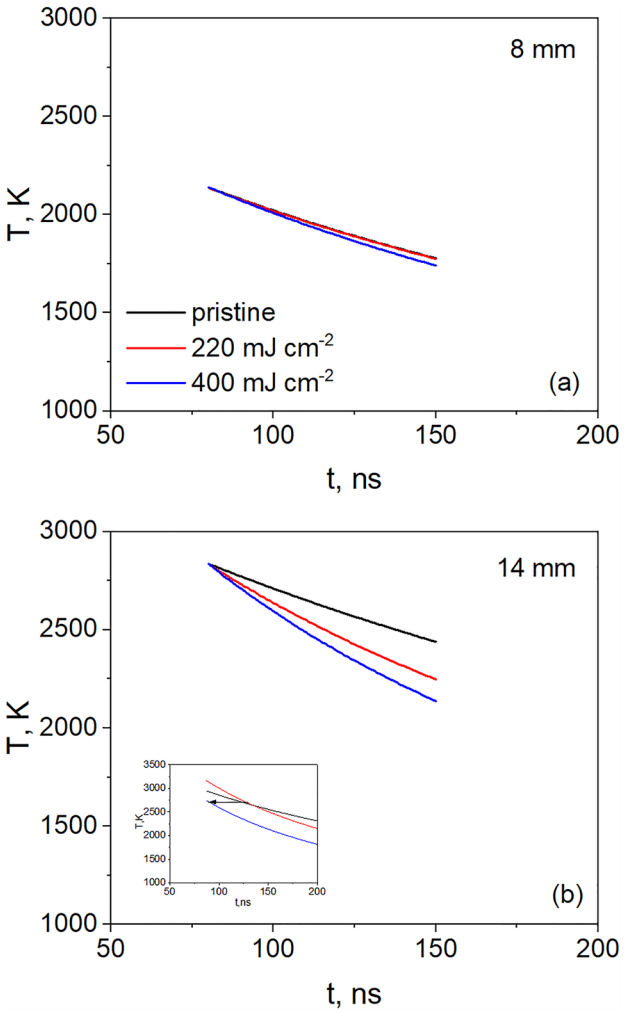

Fig. 8 Time-resolved temperature at 150 mJ cm^{-2} laser fluence of pristine and pre-irradiated nanoparticles at 220 mJ cm^{-2} and 400 mJ cm^{-2}. Results for particles sampled at 8 mm (**a**) and 14 mm (**b**) height above the burner. The insert in (**b**) shows the original temperature decay curves

While for particles sampled at 8 mm (Fig. 8a) time-resolved temperature curves are quite overlapped, at 14 mm (Fig. 8b) an increase in the decay rate is observed comparing pristine and pre-irradiated particles. For clarity, the original temperature decay curves at 14 mm are reported in the insert in Fig. 8b. According to the literature [1], the temperature decay rate depends on the particle diameter and the thermal accommodation coefficient, which represents the heat transfer efficiency between surface and gas after collision. If one considers the change of this last parameter weakly affected by laser irradiation, a decrease in the particle dimension has to be considered to justify this increase in the temperature decay rate.

Our findings are also supported by the works in [27], and in particular by measurements carried out in a premixed flame. These authors found that sublimation temperature of carbon particles depends on their size and structure. An increase in the sublimation temperature from 2700 to 4500 K is correlated to the increasing of particle dimension from 12 to 23 nm. Therefore, the reduction of the temperature at the plateau regime that we observed for mature pre-irradiated particles confirms the formation of new smaller particles and having internal structure different from the original ones. These results underline the importance of considering the change in the optical and thermodynamic properties of the carbon nanoparticles in the application of diagnostic techniques.

6 Conclusions

Extinction and two-color LII measurements are carried out on pristine and pre-irradiated nanoparticles to investigate the effects of laser irradiation on their properties. In particular, wavelength-resolved extinction data are used to deduce pyrometric temperatures during LII measurements.

To this purpose, the study was performed on particles sampled from a premixed flame at different heights above the burner surface, in order to investigate the effect on particles in different aging stages.

Nascent particles exhibit no relevant changes in the spectral dependence of the absorption coefficient after pre-irradiation at different laser fluences. In line with these results, considering LII signal and peak temperature fluence curves, no changes are detected in the saturation regime, where temperature reaches a value lower than the one normally obtained for mature particles. On the contrary, in the low fluence regime, a shift of the fluence curve is detected comparing pristine and pre-irradiated nanoparticles, indicating a significant enhancement of the absorption coefficient of the pre-irradiated nanoparticles at the excitation wavelength.

In the case of mature particles, significant changes in the absorption spectra are detected increasing the pre-irradiating fluence. More specifically, an enhancement of the absorption coefficient is observed in the spectral region below 600 nm. From LII measurements, a decrease in the temperature at the plateau regime was retrieved: from 4000 K of pristine particles to 3500 K of pre-irradiated particles, being this last value close to the temperature of nascent particles at the plateau regime. Moreover, after pre-irradiation at 400 mJ cm^{-2}, nanoparticles collected at different heights exhibit similar temperature curve as well as the same spectral behavior of the absorption coefficient. In other words, mature particles pre-irradiated at relatively high laser fluences are modified in such a way that they behave as nascent particles. On the contrary of what expected, under laser irradiation mature particles undergo fragmentation and/or vaporization with subsequent formation of new particles rather than annealing.

These findings are important for understanding the processes occurring to nanoparticles under laser irradiation as well as for a suitable implementation of LII and more generally other optical diagnostic techniques.

Supplementary Information The online version contains supplementary material available at https://doi.org/10.1007/s00340-023-08078-9.

Acknowledgements The authors would like to acknowledge the financial support from the PRIN project 2017PJ5XXX: ''Modeling and Analysis of carbon nanoparticles for innovative applications Generated dIrectly and Collected During combuSTion (MAGIC DUST)''.

Author contributions F.M., S.B. and D.C. performed the experimentation. F.M., R.D. and S.D.I. performed the formal analysis, the conceptualization and the methodology. F.M. prepared the figures. S.D.I. wrote the main manuscript text. All authors reviewed the manuscript.

Funding Open access funding provided by the Cyprus Libraries Consortium (CLC).

Data availability Data can be made available upon request to the authors for further exploration or use for model validation.

Declarations

Competing interests The authors declare no competing interests.

References

1. H.A. Michelsen, C. Schulz, G.J. Smallwood, S. Will, Progr. Energ. Combust. **51**, 2–48 (2015). https://doi.org/10.1016/j.pecs.2015.07.001
2. S. De Iuliis, F. Migliorini, R. Dondè, Appl. Phys. B **125**, 219 (2019). https://doi.org/10.1007/s00340-019-7324-7
3. T.A. Sipkens, J. Menser, T. Dreier, C. Schulz, G.J. Smallwood, K.J. Daun, Appl. Phys. B **128**, 72 (2022). https://doi.org/10.1007/s00340-022-07769-z
4. T.A. Sipkens, N.R. Singh, K.J. Daun, Appl. Phys. B **123**, 14 (2017). https://doi.org/10.1007/s00340-016-6593-7
5. S. De Iuliis, F. Cignoli, G. Zizak, Appl. Opt. **44**(34), 7414 (2005). https://doi.org/10.1364/AO.44.007414
6. F. Migliorini, S. De Iuliis, S. Maffi, G. Zizak, Appl. Phys. B **120**(3), 417–427 (2015). https://doi.org/10.1007/s00340-015-6151-8
7. X. Lopez-Yglesias, P.E. Schrader, H.A. Michelsen, J. Aerosol Sci. **75**, 43–64 (2014). https://doi.org/10.1016/j.jaerosci.2014.04.011
8. R.P. Bambha, M.A. Dansson, P.W. Schrader, H.A. Michelsen, Appl. Phys. B **112**, 343–358 (2013). https://doi.org/10.1007/s00340-013-5463-9
9. G. De Falco, M. Sirignano, M. Commodo, L. Merotto, F. Migliorini, R. Dondè, S. De Iuliis, P. Minutolo, A. D'Anna, Fuel **220**, 396–402 (2018). https://doi.org/10.1016/j.fuel.2018.02.028
10. C. Betrancourt, X. Mercier, F. Liu, P. Desgroux, Appl. Phys. B **125**, 16 (2019). https://doi.org/10.1007/s00340-018-7127-2
11. R.L. Vander Wal, M.Y. Choi, Carbon (1999). https://doi.org/10.1016/S0008-6223(98)00169-9
12. R.L. Vander Wal, T.M. Ticich, A.B. Stephens, Appl. Phys. B (1998). https://doi.org/10.1007/s003400050483
13. B. Apicella, P. Pré, J.N. Rouzaud, J. Abrahamson, R.L. Vander Wal, A. Ciajolo, A. Tregrossi, C. Russo, Combust. Flame (2019). https://doi.org/10.1016/j.combustflame.2019.02.026
14. S. De Iuliis, F. Cignoli, S. Maffi, G. Zizak, Appl. Phys. B **104**, 321–330 (2011). https://doi.org/10.1007/s00340-011-4535-y
15. S. Török, M. Mannazhi, S. Bergqvist, K. Le Cuong, P.-E. Bengtsson, Aerosol Sci Tech (2022). https://doi.org/10.1080/02786826.2022.2046689
16. H.A. Michelsen, A.V. Tivanski, M.K. Gilles, L.H. van Poppel, M.A. Dansson, P.R. Buseck, Appl. Opt. **46**(6), 959–977 (2007). https://doi.org/10.1364/ao.46.000959

17. F. Migliorini, S. De Iuliis, R. Dondè, M. Commodo, P. Minutolo, A. D'Anna, *Exp* (Fluid Sci, Therm, 2020). https://doi.org/10.1016/j.expthermflusci.2020.110064
18. F. Migliorini, S. Belmuso, D. Ciniglia, R. Dondè, S. De Iuliis, Phys. Chem. Chem. Phys. **24**, 19837 (2022). https://doi.org/10.1039/d2cp02639b
19. F. Migliorini, S. Belmuso, R. Donde, S. De Iuliis, Phys. Chem. Chem. Phys. **23**, 15702 (2021). https://doi.org/10.1039/d1cp01267c
20. F. Migliorini, S. Belmuso, R. Dondè, S. De Iuliis, I. Altman, Carbon Trends (2022). https://doi.org/10.1016/j.cartre.2022.100184
21. A. Bescond, J. Yon, F.-X. Ouf, C. Rozè, A. Coppalle, P. Parent, D. Ferry, C. Laffon, J. Aerosol Sci. **101**, 118 (2016)
22. F. Migliorini, S. De Iuliis, S. Maffi, G. Zizak, Appl. Phys. B **112**, 433–440 (2013). https://doi.org/10.1007/s00340-013-5385-6
23. F. Migliorini, K.A. Thomson, G.J. Smallwood, Appl. Phys. B **104**, 273–283 (2011). https://doi.org/10.1007/s00340-011-4396-4
24. N.E. Olofsson, J. Simonsson, S. Török, H. Bladh, P.E. Bengtsson, Appl. Phys. B **119**, 669–683 (2015). https://doi.org/10.1007/s00340-015-6067-3
25. F. Liu, D.R. Snelling, K.A. Thomson, G.J. Smallwood, Appl. Phys. B **96**, 623–636 (2009). https://doi.org/10.1007/s00340-009-3560-6
26. F. Liu, G.J. Smallwood, Combust Science Technol. **195**, 144–158 (2019). https://doi.org/10.1080/00102202.2019.1678837
27. E.V. Gurentsov, A.V. Drakon, A.V. Eremin, R.N. Kolotushkin, EYu. Mikheyeva, Tech. Phys. **92**(1), 53–60 (2022). https://doi.org/10.21883/TP.2022.01.52533.206-21